Solid State Ionics 206 (2012) 39–44

Contents lists available at SciVerse ScienceDirect

Solid State Ionics

journal homepage: www.elsevier.com/locate/ssi

Preparation of compact Li-doped $Y_2Ti_2O_7$ solid electrolyte

L.C. Wen [a], H.Y. Hsieh [a], Y.H. Lee [a], S.C. Chang [a], H.-C.I. Kao [a,*], H.S. Sheu [b], I.N. Lin [c], J.C. Chang [d], M.C. Lee [e], Y.S. Lee [e]

[a] Department of Chemistry, Tamkang University, Tamsui 25137, Taiwan
[b] National Synchrotron Radiation Research Center, Hsinchu 30076, Taiwan
[c] Department of Physics, Tamkang University, Tamsui 25137, Taiwan
[d] Solar Technology, Inc. Tainan 70955, Taiwan
[e] Institute of Nuclear Energy Research, Atomic Energy Council, Longtan 32546, Taiwan

ARTICLE INFO

Article history:
Received 22 August 2010
Received in revised form 19 September 2011
Accepted 23 October 2011
Available online 26 November 2011

Keywords:
$(Y_{2-x}Li_x)Ti_2O_{7-x}$
Pyrochlore
Titanate
Li_2O
Oxygen ion conductor

ABSTRACT

Three series of solid electrolytes were prepared with the nominal compositions of $(Y_{2-x}Li_{3x})Ti_2O_7$ (Y3LT), $(Y_{2-x}Li_x)Ti_2O_{7-x}$ (YLT) and $Y_{2-x}Ti_2O_{7-3x/2}$ (YT) with $x = 0.040 - 0.11$. Comparing the unit cell *a*-axis of the YLT with that of YT, the latter is shorter with the same amount of x. This indicates a successful substitution of the Li ion into the Y site of $Y_2Ti_2O_7$. However, both Y3LT and YLT have exactly the same unit cell *a*-axis length with the same amount of x so that the solid solution formed probably has the same formula, $(Y_{2-x}Li_x)Ti_2O_{7-x}$, in which only one Li ion is substituted into the Y site. Extra Li_2O added in the Y3LT is probably acting as a self flux to lower the melting point of the mixture. As a result, materials become more compact and grains grow bigger. One compound of Y3LT with $x = 0.060$ has a total conductivity of 4.3 (4) $\times 10^{-4}$ S·cm^{-1} at 700 °C. Adding Li_2O as a flux and carefully controlling the heat treatment history, compact sample of Y3LT with a relative density higher than 90% was obtained at a temperature as low as 1150 °C. Its ionic conductivity is comparable to one $Y_2Ti_2O_7$ prepared at 1600 °C with a conductivity reported as 2.30×10^{-4} S·cm^{-1}.

1. Introduction

Solid oxide fuel cell (SOFC) is an electrochemical system that generates electricity directly from oxidizing a fuel. A single cell consists of porous anode and cathode, and a dense layer of solid electrolyte in between [1–5]. All of them are stacked together and are less than a millimeter thick. In order to prepare a compact electrolyte, the sintering temperature is generally high. For example, YSZ (yttria−stablized −zirconia) and GDC (Gd-doped ceria), both of them require 1450 °C sintering temperature and several hours heat treatment period for achieving dense materials [6,7]. Both YSZ and GDC have a fluorite (AO_2) phase [8]. They are used as electrolytes in the SOFC. Pyrochlore has a formula of $A_2B_2O_7$, which is a superstructure derivative of the simple fluorite phase [9]. For every four units of AO_2, there is an oxygen vacancy [10]. Both $Ln_2Zr_2O_7$ and $Ln_2Ti_2O_7$ (Ln = rare earth cation) are possible candidates as electrolytes in the SOFC [1,4,11]. High temperatures are required to prepare compact samples. $Ln_2(Zr,M)_2O_7$ (Ln = La, Nd, Sm, Gd and Er; M = Y, Ti, In and Mg) pyrochlore materials were sintered at 1650 °C and they have a relative density higher than 95% [11]. $Lu_2Ti_2O_7$ was sintered at 1400 °C or 1700 °C for 10 h to achieve 92.5% or 93% dense ceramics, respectively [1].

Adding flux to reduce sintering temperature is one of the options for preparing compact solid electrolyte materials. That is an application of the eutectic property. Many literature reports dealing about the way of fabricating solid electrolytes and some of them are listed as follows. Adding 0.5 mol% of $Sr_2Ga_2O_5$ as a sintering aid in the preparation of 20SDC ($(Ce_{0.8}Sm_{0.2})O_{1.9}$), 1250 °C is high enough to obtain a pellet with a relative density of 97%. Nevertheless, without $Sr_2Ga_2O_5$, 1550 °C is required to obtain the same pellet [12]. Adding 0.5 wt.% cobalt metal powder as a flux, at 1300 °C, relative density of 10SDC ($(Ce_{0.9}Sm_{0.1})O_{1.95}$) reaches to 96%, instead, without flux, sintering at 1400 °C, relative density is 91% [13]. Adding 0.5 mol% Ga_2O_3 into 20GDC, at 1300 °C, 94% relative density is achieved [14]. Besides, the flux could be used as a scavenger to decrease grain boundary resistance [13,15]. However, the existence of the second phase would probably decrease the conductivity of the electrolyte if it hinders the transportation of the ions [16].

In our previous report, Li_2O was added into $Y_2Ti_2O_7$ to prepare $(Y_{2-x}Li_x)Ti_2O_{7-x}$ solid electrolyte with a solid state reaction method. Samples were heat treated at 1180 °C and the relative density is only in the range of 50 to 60% which is too low to be used as a solid electrolyte. Therefore, no ionic conductivity was measured [17]. On the other hand, Yamaguchi et al. prepared $Y_2Ti_2O_7$ at 1600 °C, which is dense enough for the electrical measurement [18].

In this report, compact $(Y_{2-x}Li_x)Ti_2O_{7-x}$ was prepared at temperature as low as 1150 °C. Relative density is increased to more

* Corresponding author at: Department of Chemistry, Tamkang University, Tamsui 25137, Taiwan. Tel.: +886 2 2625 1661; fax: +886 2 2620 9924.
E-mail address: kaohci@mail.tku.edu.tw (H.-C.I. Kao).

0167-2738/$ – see front matter © 2011 Elsevier B.V. All rights reserved.
doi:10.1016/j.ssi.2011.10.021

than 90%. Ionic conductivity and transference number at different temperatures, as well as oxygen partial pressures were investigated. Li ion has a valence of 1+, replacing one atom of Y^{3+} by one Li^{+} ion, one oxygen vacancy is created. Ionic conductivity is generally increased with increasing the carrier vacancy. In addition, among the alkaline oxides, Li_2O is the least volatile one. In order to keep alkaline cation in the sample, Li_2O is the best candidate.

2. Experimental

Nominal compositions of the materials prepared were $(Y_{2-x}Li_{3x})Ti_2O_7$ (Y3LT), $(Y_{2-x}Li_x)Ti_2O_{7-x}$ (YLT) and $Y_{2-x}Ti_2O_{7-3x/2}$ (YT) with $x = 0.040 - 0.11$. Appropriate amount of 99.99% of Y_2O_3 (Strem), 99% of TiO_2 (Junsei), Li_2CO_3 (Merck) and PMMA (poly (methyl methacrylate)) were weighed and ball milled for 24 h with zirconia balls in acetone. The dried fine powder obtained was pelletized by a uniaxial press with 840 MPa pressure and then heat treated with a series of temperature programming steps for the Y3LT and YLT samples and 1150 °C for 10 h is fine for preparing dense materials, but in order to make the YT series, higher temperature and longer time were needed. They were prepared at 1200 °C for 36 h. Ceramic samples were cooled in the furnace by turning off the electric power. It is assumed that the Y3LT has one mole of Li ion doped into the Y site and two moles of the Li_2O act as self flux to enhance the relative density of the samples [17]. Weight percent of the Li_2O employed as flux was listed in Table 1. They are between 0.31 and 0.88% when x varies from 0.040 to 0.11, respectively. In the YLT series, it is assumed that all the Li ions are doped into the Y site. In the YT series, there is a Y deficiency of the Y site that is prepared for comparison with the Y3LT and YLT in order to understand whether Li ion is doped into the crystal lattice.

The relative density of the sintered specimens was measured by the Archimedes method using de-ionized water as a liquid medium. Powder diffraction data used for the Rietveld refinement were collected on the BL01C2 beam line at the National Synchrotron Radiation Research Center (NSRRC) in Taiwan and operated at ring energy of 1.5 GeV and 300 mA. Powder diffraction patterns were recorded by a Mar345 imaging plate area detector with the X-ray wavelength of 0.495941 Å (25 keV). The GSAS (General Structure Analysis System) program developed by Larson and von Dreele was employed for the structural parameters analysis with the Rietveld method [19]. In the beginning of the Rietveld refinement, thermal parameter, U_{iso}, was set as 0.025 $Å^2$ for all the atomic sites. All three oxygen sites are constrained to the same U_{iso} and they are not allowed to vary independently because of the light mass of the oxygen atom compared to other atoms in the sample. Morphology of the sample was observed with a VEGA\\SBH Scanning Electron Microscope.

Electrical parameters were determined by the AC impedance spectroscopy (EIS) using fully automated Autolab PGSTAT30 Potentiostat/Galvanostat system in air in the frequency range from 1 Hz to 1 MHz with a density of 10 points/decade and the excitation amplitude of 50 mV in the temperature range from 450 to 700 °C. Pellet samples were measured by a two-probe method with Pt electrodes and Ag paste. An R-type thermocouple was attached near the sample to measure the temperature. Electrical conductivity with respect to the partial pressure of oxygen was also measured by the EIS spectroscopy. Different amount of oxygen and nitrogen gas were allowed to flow into the sample chamber simultaneously to control the oxygen partial pressure. Percentage of the oxygen gas varied from 10% to 100%. The flow rates were fixed by a mass flow controller to a total rate of 100 sccm. The electromotive forces (EMFs) were measured on an oxygen concentration cell, in which ambient air was employed as a reference and a mixed gas, 50% oxygen and 50% nitrogen, was introduced to another side of the cell. The whole system was allowed to stabilize under each condition before the measurement.

Table 1
The wt.% of the extra Li_2O added into the Y3LT series.

x	0.040	0.050	0.060	0.070	0.080	0.090	0.10	0.11
wt.%	0.31	0.39	0.47	0.55	0.63	0.71	0.80	0.88

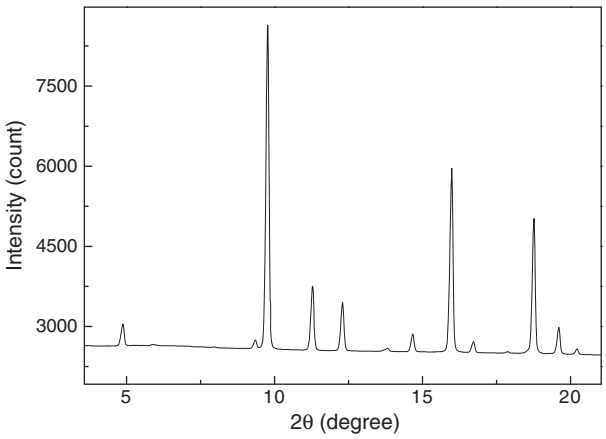

Fig. 1. XRD pattern of the Y3LT with x = 0.060. Wavelength of the X-ray beam is 0.495941 Å.

3. Results and discussion

All three series, Y3LT, YLT and YT from x = 0.040 to x = 0.11, have single phase XRD patterns and no impurity is observed. If there is Li_2O coexistence with $(Y_{2-x}Li_x)Ti_2O_{7-x}$, it cannot be detected due to the low reflecting power of the Li ion to the X-ray. One typical example is shown in Fig. 1, which is the XRD pattern of the Y3LT with x = 0.060. Wavelength of the X-ray beam is 0.495941 Å, which is about three times shorter than the common X-ray source of the Cu Kα radiation (1.5418 Å) so that the diffraction angles in Fig. 1 are about one third of the 2θ angles found in several literature reports [20,21]. The unit cell parameters of all samples were determined by the Rietveld refinement method. One refined result for the $(Y_{2-x}Li_{3x})Ti_2O_{7-x}$ with x = 0.060 is shown in Fig. 2, which includes the experimental, calculated, and difference XRD profiles. Crosses are the experimental data; solid lines are the calculated profiles. All the possible Bragg reflections are indicated with short vertical tics below the calculated

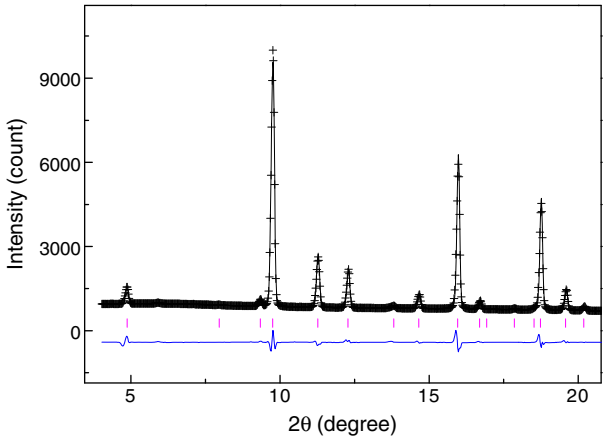

Fig. 2. Rietveld refinement result of the Y3LT with x = 0.060. The figures include the experimental, calculated, and difference XRD profiles. Crosses are the experimental data; solid lines are the calculated profile. All the possible Bragg reflections are indicated with short vertical tics below the calculated profile. The difference between the experimental and calculated results is plotted below the Bragg reflection tic. Wavelength of the X-ray beam is 0.495941 Å.

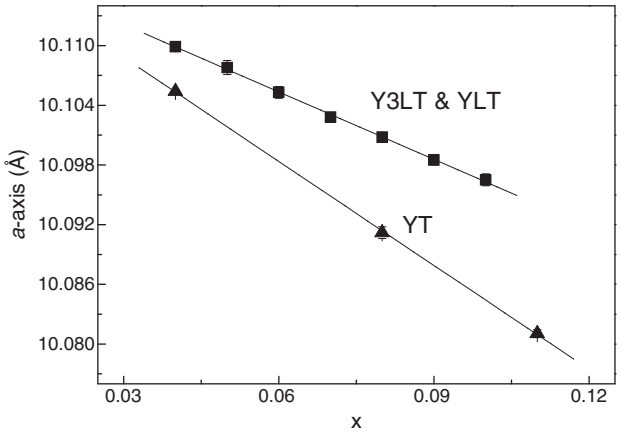

Fig. 3. Unit cell *a*-axes of the (■) Y3LT, (●) YLT and (▲) YT series with the amount of x. Standard deviations are included.

profiles. The difference between the experimental and calculated results is plotted below the Bragg reflection tics.

The *a*-axis of these samples with respect to the amount of substitution, x is plotted in Fig. 3. The unit cell parameters vary linearly with the amount of x. They obey the Vegard's law well. For the Y3LT and YLT, they have the same *a*-axis with the same amount of x. It indicates that they have the same amount of Li ion doped into samples. Therefore, both series have the same chemical formula, $(Y_{2-x}Li_x)Ti_2O_{7-x}$. The extra Li_2O added into the Y3LT series probably acts as a self flux to increase the grain size and the relative densities of all samples, as shown in Figs. 4 and 5. Unit cell *a*-axis of the YT series are shorter than the Y3LT and YLT with the same amount of x that is probably caused by the deficiency of the Y site cation. On the other hand, Li ions are doped into Y site to increase the unit cell parameters of YLT and Y3LT so that their *a*-axes are longer than their counterparts, the YT series with the same amount of x. Ionic radii of 8-coordination Y^{3+} and Li^{+} are 1.109 and 0.92 Å [22], respectively. A linear decrease of the *a*-axis length in the YLT series is also an indirect proof of the incorporation of the Li ion into Y site in the pyrochlore phase. In the Rietveld refinement calculation, all of the R_{wp} and R_p obtained are less than 5 and 2.5%, respectively and the χ^2 is between 0.09 and 1.6. All of them are acceptable and the results are believable.

In the preparation of the Y3LT and YLT samples, the temperature was held at 600 °C for 2 h, 675 °C for 6 h, 1150 °C for 10 h, slow cooling to 800 °C and then cooling in the furnace by turning off the furnace power. During the thermal history, PMMA was first decomposed, and then Li_2CO_3 was decomposed to Li_2O. Both YLT and Y3LT were sintered at 1150 °C. However, in the preparation of the YT samples, the same conditions were first used, but impurity was observed in the sample's XRD pattern. In addition, the resulting samples were porous. Therefore, the temperature was raised to 1200 °C and held for 36 h to prepare the YT samples. Single phased materials were then obtained, but their relative density was still too low to carry out electrical measurement. They must be less than 60% dense. Adding Li_2O into YLT and Y3LT indeed helps to accelerate the formation of the $(Y,Li)_2Ti_2O_7$ pyrochlore phase.

Microstructure of the Y3LT and YLT examined by SEM are shown in Fig. 4; 4(a) and 4(b) is the YLT samples with x = 0.060 and 0.11, respectively and 4(c) and 4(d) are taken from the Y3LT with the same amount of x. For the YLT samples, which are a solid solution

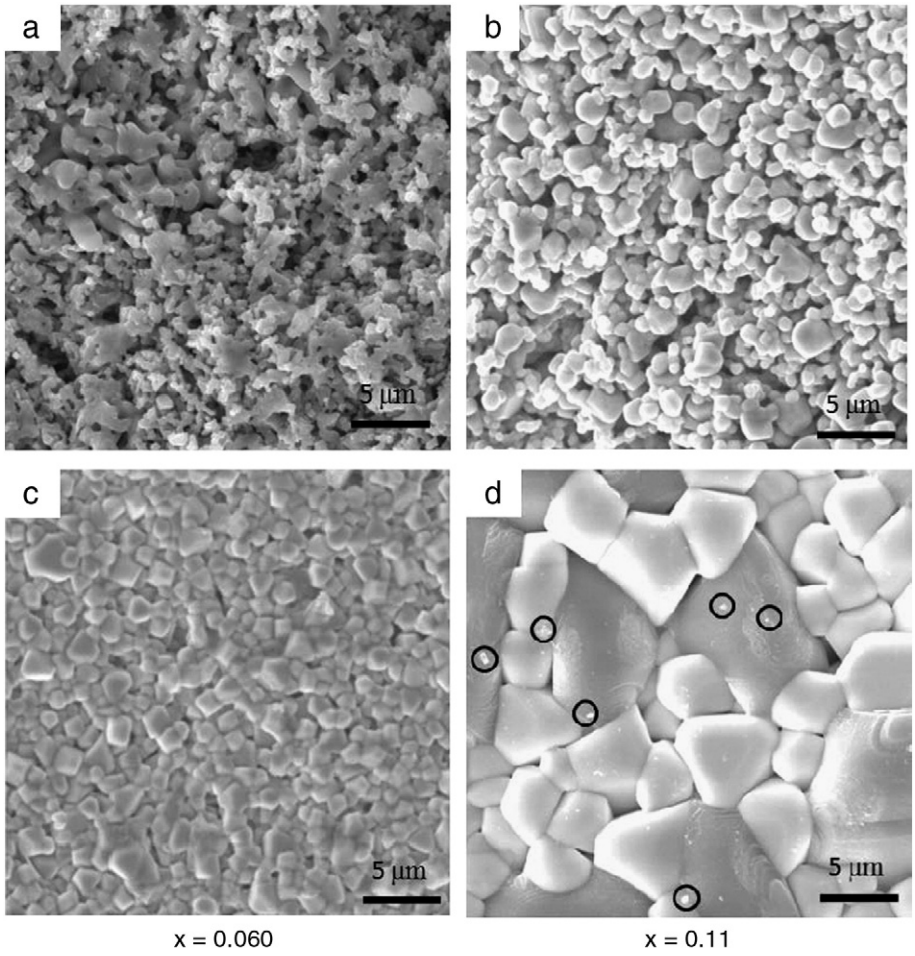

Fig. 4. Morphology of the YLT with x = (a) 0.060, (b) 0.11; the Y3LT with x = (c) 0.060, and (d) 0.11 examined by SEM.

of the $Y_2Ti_2O_7$ and Li_2O. The melting point of the solid mixture is always lower than the pure materials. Increasing the amount of Li_2O, the depression of the melting point is enhanced so that grains grow better in the samples with x = 0.11 than that in the x = 0.060. Relative density is also increased with increasing the amount of x shown in Fig. 5. That is another evidence of melting point depression. Looking into Fig. 4(c) and (d), x = 0.060 and 0.11, respectively, grain size increases with increasing x, because the amount of extra Li_2O is further increased (see Table 1). Li_2O acting as a self flux to decrease the melting point of the mixture. Comparing Y3LT with YLT for the same amount of x, both grain size and relative density of the former are larger than the latter. In Fig. 4(d), tiny particles on the surface of the Y3LT are observed. They are marked by circles, which are probably caused by the extra Li_2O. However, no second phase is found in the YLT samples in Fig. 4(b), in this case, all the Li_2O are probably soluble into $Y_2Ti_2O_7$.

Relative density of the Y3LT and YLT measured by the Archimedes method is plotted in Fig. 5. Relative density of the YT series is too low to be measured so that they are not shown. For the YLT series, they are in between 60 and 80%. Relative density increases with an increasing amount of Li content in the sample due to the lowering of the melting point by the addition of more Li_2O. The more is the amount of Li_2O, the lower is the melting point of the mixture. For the Y3LT series, all samples have a relative density higher than 90%. In this series, extra Li_2O is added as a flux, melting point of the mixture is further decreased and the relative density is higher than YLT series. The wt.% of the Li_2O as a flux is listed in Table 1. They are in the range of 0.31 to 0.88%. The Y3LT with x = 0.050, relative density is 95%. The amount of extra Li_2O is 0.39%. It seems that 0.4% of extra Li_2O is a sufficient amount to obtain compact solid electrolyte of $(Y_{2-x}Li_x)Ti_2O_{7-x}$.

Typical impedance Cole—Cole plots (Nyquist diagrams) obtained from Pt|Y3LT|Pt are presented in Fig. 6(a) and (b) at 547 and 648 °C, respectively in the ambient pressure for a Y3LT sample with x = 0.060. The impedance data can be interpreted by using an equivalent circuit model of the form $(R_b//C_b)(R_{gb}//C_{gb})$ where the bulk (b) and grain boundary (gb) contributions are in series, and R and C in parallel accounts respectively for the corresponding resistance and universal capacitance values of each contribution [23] at 500 °C where the R_b is the bulk resistance at higher frequency semicircle and R_{gb} is the grain boundary one at lower frequency semicircle shown in Fig. 6(a). At higher temperature, only the grain boundary semicircle is observed, the equivalent circuit model of the form $R_b(R_{gb}//C_{gb})$ was employed for the calculation shown in Fig. 6(b). Conductivity of the Y3LT at different temperatures is listed in Table 2. Conductivity at 500 °C is in the order of 10^{-5} S·cm^{-1}, which increases to $4.3(4)\times10^{-4}$ S·cm^{-1} at 700 °C for the Y3LT with x = 0.060. That is higher than the $Y_2Ti_2O_7$ measured at the same temperature by different research groups [18,24]. It has

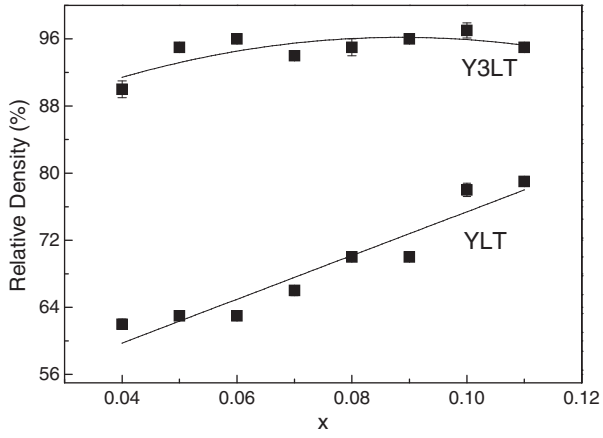

Fig. 5. Relative density of the Y3LT and YLT vs. x. Standard deriations are included.

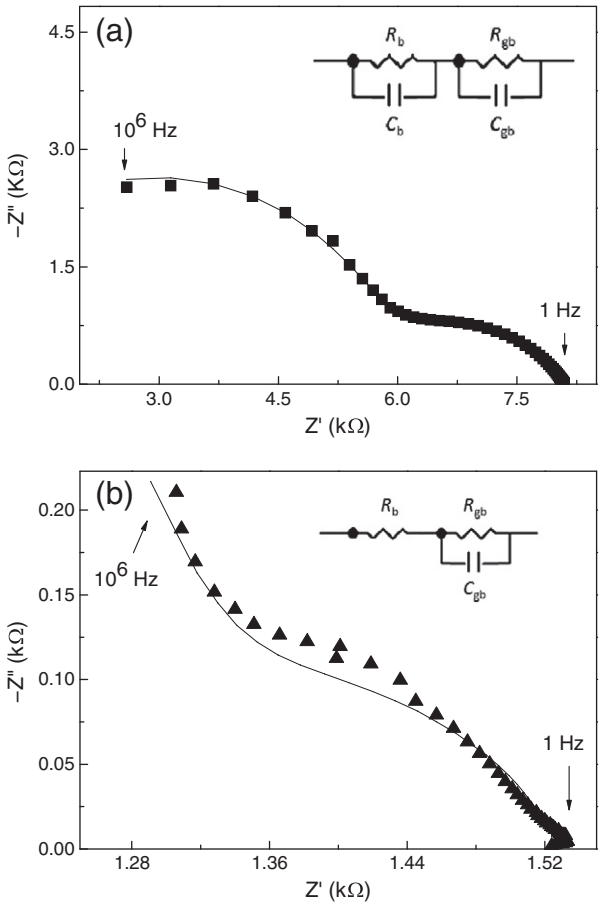

Fig. 6. Complex impedance plot obtained at (a) 547 °C, (b) 648 °C for the Y3LT sample with x = 0.060. The equivalent circuit model is shown in the figures.

conductivity in the range of $1.67-2.30\times10^{-4}$ S·cm^{-1}. Yamaguchi et al. [18] prepared $Y_2Ti_2O_7$ sample at 1600 °C for 10 h. The sample has total conductivity of 2.30×10^{-4} S·cm^{-1}. Comparing the results found in our samples, introducing Li_2O as a flux, Y3LT prepared at 1150 °C has a conductivity at the same level as the $Y_2Ti_2O_7$ sintered at 1600 °C although the second phase is probably present in the Y3LT sample shown in Fig. 4. That does not seem to affect the conductivity of Y3LT sample. Adding Li_2O as a flux, preparation temperature has been lowered dramatically. Obviously, Li_2O is an effective flux for making $Y_2Ti_2O_7$ solid electrolyte. By introducing Li ion into $Y_2Ti_2O_7$, unit cell *a*-axis is decreased, which is not favored as the ionic conductivity is concerned. Nevertheless, oxygen vacancies are increased in the meanwhile so that ionic conductivity is probably compensated. As a consequence, conductivity is not affected by slightly shrinking the unit cell parameters.

Table 2
Electrical conductivity of the Y3LT with x = 0.060 measured at different temperatures.

Temperature (°C)	σ_{total} (S·cm^{-1})
453	$3.7(2)\times10^{-6}$
484	$7.4(2)\times10^{-6}$
500	$1.32(4)\times10^{-5}$
547	$2.36(8)\times10^{-5}$
570	$3.7(2)\times10^{-5}$
600	$5.8(3)\times10^{-5}$
621	$8.5(6)\times10^{-5}$
648	$1.3(1)\times10^{-4}$
674	$1.8(1)\times10^{-4}$
700	$4.3(4)\times10^{-4}$

*Parentheses are the standard deviation of the measurement.

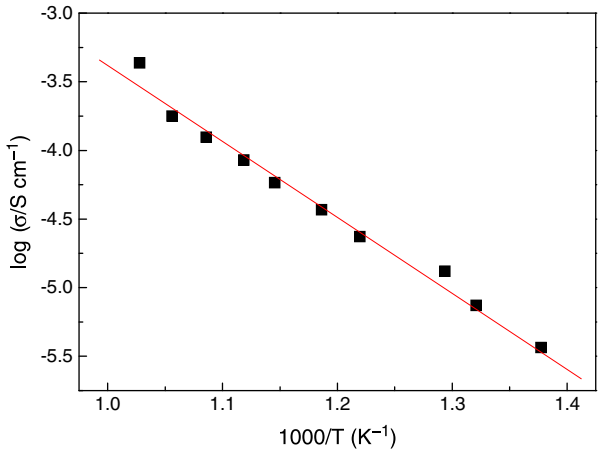

Fig. 7. Arrhenius plot of the total conductivity for the Y3LT with x = 0.060.

Fig. 7 is the Arrhenius plot of the total conductivity (σ_b plus σ_{gb}) of the Y3LT with x = 0.060, which follows the Arrhenius behavior quite well, the correlation value for the linear least square simulation is 0.998, very close to 1, it indicates that the ionic diffusion process is thermally activated [25]. The activation energy (E_a) of the oxygen ion transport is 1.08(5) eV, which was calculated by taking the slope of this plot into Arrhenius equation. Activation energy obtained by Uematsu et al. [24] and Yamaguchi et al. [18] for the $Y_2Ti_2O_7$ is 1.00 [24] and 0.86 eV [18], respectively. Our result is quite close to that obtained by Uematsu. For the oxides with a similar structure, such as, GDC ($(Gd_{0.2}Ce_{0.8})O_{2-\delta}$) and SDC ($(Sm_{0.2}Ce_{0.8})O_{2-\delta}$) investigated by Kumar et al. [26] and Fu [27], their E_a are 1.09 and 0.85 eV, respectively. Both GDC and SDC have a fluorite phase [8]. $Y_2Ti_2O_7$ has a pyrochlore phase, which is a superstructure of fluorite phase [9]. In general, activation energy for these fluorites or pyrochlores is near 1 eV.

Fig. 8 presents the frequency as a function of the real and imaginary parts of the impedances measured on the Y3LT with x = 0.060. Impedance decreases with increasing frequency for all the curves measured at different temperatures in Fig. 8(a) and (c). This phenomenon is typical for the ionic conductors. The impedance Z′ values at higher frequency for all temperatures indicate a possible release of space charge [28,29]. The shape of the curve obtained at 500 °C is slightly different than the one obtained at 700 °C. Due to the shape difference in the Nyquist diagram shown in Fig. 6. In Fig. 8(b), two relaxation peaks are observed for curves obtained at the temperatures ≤547 °C. Peak positions shift toward higher frequencies when the measuring temperatures are increased. That is assumed due to the higher oxide ion conductivity in the target compound in this study. The relaxation peak profile also becomes broader when the measuring temperature is increased.

Fig. 9 is the total ionic conductivity as a function of the oxygen partial pressures for the Y3LT with x = 0.060. When the measuring temperature is at 500 °C, conductivities do not change with respect to the oxygen partial pressures varied from 10% to 100%. In other words, the sample has pure oxide ion conductivity at 500 °C. At 700 °C, conductivity does not change if the oxygen partial pressure is less than 60%. For higher oxygen pressures, conductivities increase gradually. The Y3LT with x = 0.060 becomes a p-type semiconductor that means the sample has electronic conduction contribution at this temperature [30].

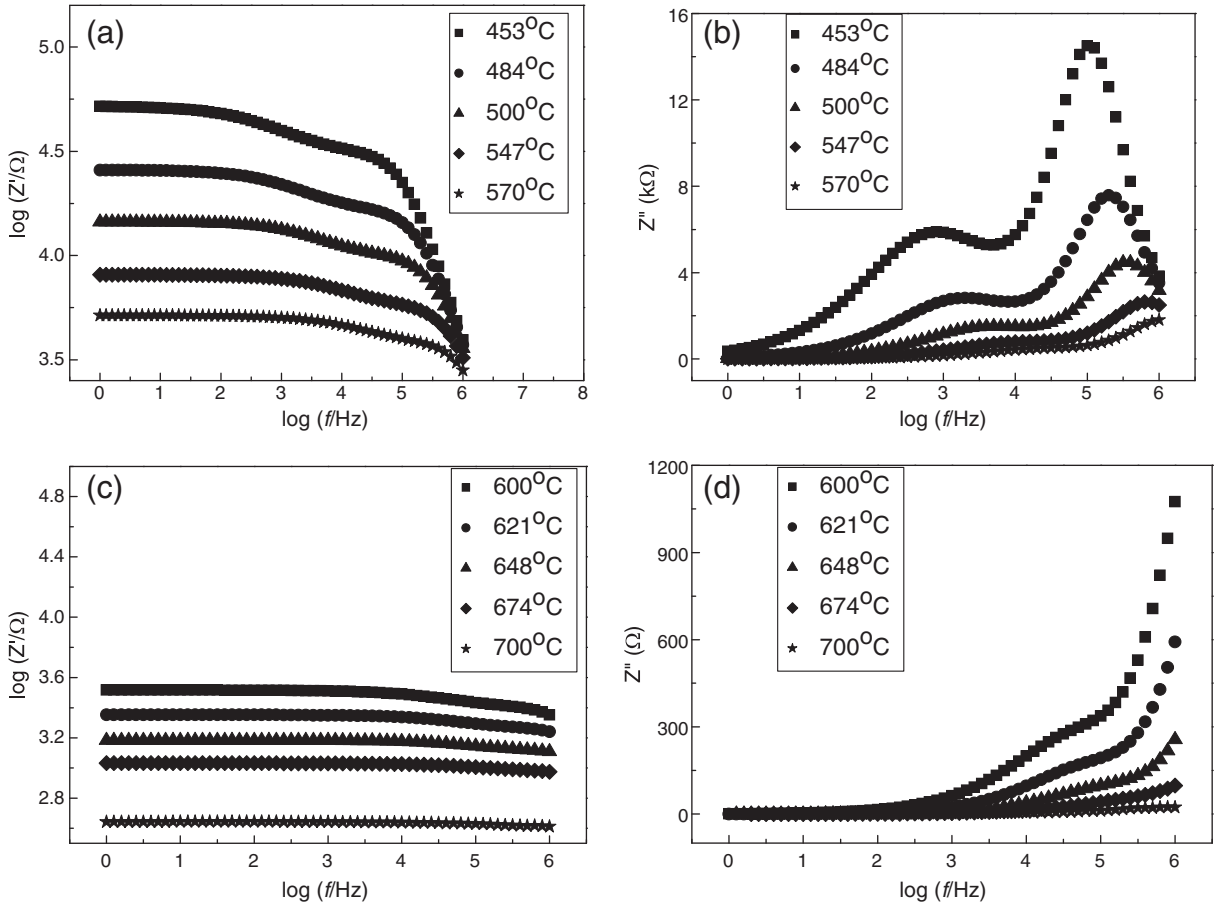

Fig. 8. Log−log representation of the real part, (a) and (c), and the imaginary part, (b) and (d), of the resistance vs. frequency at temperatures ≤570 °C, shown in (a) and (b), and at temperatures ≥600 °C, shown in (c) and (d), for the Y3LT with x = 0.060.

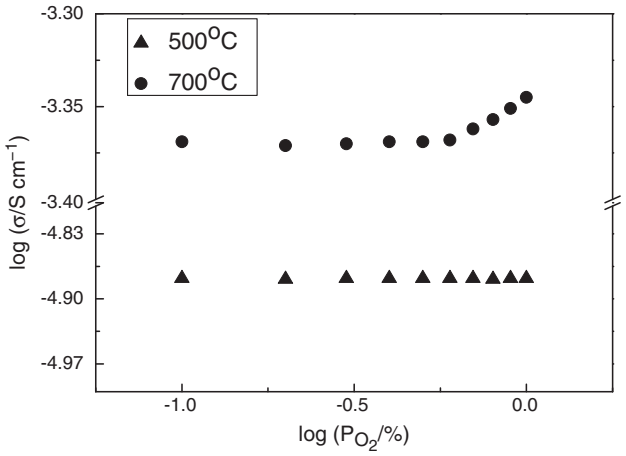

Fig. 9. The total electrical conductivity as a function of the oxygen partial pressures measured at 500 and 700 °C for the Y3LT with x = 0.060.

Table 3
The theoretical and experimental EMF, transference number of the ionic conduction of the Y3LT with x = 0.060 measured at 500, 600 and 700 °C.

Potential	Temperature (°C)		
	500	600	700
E_{theory} (mV)	14.45	16.31	18.18
E_{obs} (mV)	14.40	14.88	13.07
t_i	1.00	0.91	0.72

In order to understand the contribution from electronic conduction in every operating temperature, the EMF (electromotive force) was measured at 500, 600 and 700 °C. The mixing gases consisting of 50% oxygen and 50% nitrogen were introduced to one side of the oxygen concentration cell, and another side was exposed in ambient air as a reference. The theoretical potential can be given by using Nernst equation for the oxygen concentration cell [31]. In this study, the transference number is 0.99 at 500 °C for the Y3LT with x = 0.060. It means that the electrolyte material has nearly pure ionic conductivity at this temperature. Ionic transference number decreases gradually with increasing operating temperature shown in Table 3. At 600 and 700 °C, they are 0.91 and 0.72, respectively. The fraction of the electronic conduction is 0.09 and 0.28, respectively. The major contribution of the electronic conductivity is probably coming from the Ti-atom. It is possible to have mixed valence of Ti at high temperature and the material becomes a p-type semiconductor. $Y_2Ti_2O_7$ is well known as a mixed ionic-electronic conductor [18,24,32]. Ionic transference number of the $Y_2Ti_2O_7$ reported by Kobayashi et al. also decreased with increasing temperature [32].

4. Conclusions

Li ion can be doped into the Y site of the $Y_2Ti_2O_7$ pyrochlore structure. Extra Li_2O acts as a self flux to help the densification of the Y3LT materials at 1150 °C. All of them have more than 90% relative density and the conductivity of Y3LT with x = 0.060 is as good as one $Y_2Ti_2O_7$ prepared at 1600 °C. The electrical conductivity as a function of oxygen partial pressure and the EMF measurement confirm that the Y3LT with x = 0.060 is a nearly pure oxide ion conductor at 500 °C, but it becomes mixed conductor when the operation temperature is increased.

Acknowledgment

This work is supported by the Institute of Nuclear Energy Research, Atomic Energy Council of Taiwan under the contract no. of 1002001INER055.

References

[1] A.V. Shlyakhtina, L.G. Shcherbakova, A.V. Knotko, A.V. Steblevskii, J. Solid State Electrochem. 8 (2004) 661–667.
[2] S.C. Singhal, Solid State Ion. 135 (2000) 305–313.
[3] X. Huang, H. Zhao, W. Shen, W. Qiu, W. Wu, J. Phys. Chem. Solids 67 (2006) 2609–2613.
[4] Z.G. Liu, J.H. Ouyang, Y. Zhou, X.L. Xia, J. Power, Sources 185 (2008) 876–880.
[5] Q.A. Huang, R. Hui, B. Wang, J. Zhang, Electrochim. Acta 52 (2007) 8144–8164.
[6] W. Bao, W. Zhu, G. Zhu, J. Gao, G. Meng, Solid State Ion. 176 (2005) 669–674.
[7] Y.J. Leng, S.H. Chan, S.P. Jiang, K.A. Khor, Solid State Ion. 170 (2004) 9–15.
[8] M. Yashima, M. Kakihana, M. Yoshimura, Solid State Ion. 86–88 (1996) 1131–1149.
[9] B.J. Wuensch, K.W. Eberman, C. Heremans, E.M. Ku, P. Onnerud, E.M.E. Yeo, S.M. Haile, J.K. Stlick, J.D. Jorgensen, Solid State Ion. 129 (2000) 111–133.
[10] M.E. Rabanal, A. VaÂrez, U. Amador, E.A. Dompablo, F.G. Alvarado, J. Mater. Process. Technol. 92–93 (1999) 529–533.
[11] T. Shimura, M. Komori, H. Iwahara, Solid State Ion. 86–88 (1996) 685–689.
[12] J.S. Lee, K.H. Choi, M.W. Park, Y.G. Choi, J.H. Mun, J. Alloys Compd. 474 (2009) 219–222.
[13] J. Ayawanna, D. Wattanasiriwech, S. Wattanasiriwech, P. Aungkavattana, Solid State Ion. 180 (2009) 1388–1394.
[14] T.S. Zhang, J. Ma, Y.J. Leng, Z.M. He, J. Cryst. Growth 274 (2005) 603–611.
[15] T.S. Zhang, J. Ma, L.B. Kong, S.H. Chan, P. Hing, J.A. Kilner, Solid State Ion. 167 (2004) 203–207.
[16] H.N. Kim, H.J. Park, G.M. Choi, J. Electroceram. 17 (2006) 793–796.
[17] W.P. Su, Y.H. Lee, C.T. Hsieh, H.S. Sheu, J.F. Lee, Y.P. Chiang, H.-C.I. Kao, J. Chin. Chem. Soc. 56 (2009) 1112–1117.
[18] S. Yamaguchi, K. Kobayashi, K. Abe, S. Yamazaki, Y. Iguchi, Solid State Ion. 113 (1998) 393–402.
[19] A.C. Larson, R.B. von Dreele, General Structure Analysis System; Report La-UR-86-748, Los Alamos National Laboratory, Los Alamos, 2003.
[20] A.F. Fuentes, K. Boulahya, M. Maczka, J. Hanuza, U. Amador, Solid State Sci. 7 (2005) 343–353.
[21] K.J. Moreno, R.S. Rodrigo, A.F. Fuentes, J. Alloys Compd. 390 (2005) 230–235.
[22] R.D. Shannon, C.T. Prewitt, Acta Crystallogr. A32 (5) (1976) 751–767.
[23] J.A. Díaz-Guillén, M.R. Díaz-Guillén, K.P. Padmasree, A.F. Fuentes, J. Santamaría, C. León, Solid State Ion. 179 (2008) 2160–2164.
[24] K. Uematsu, J.K. Shinozaki, O. Sakurai, N. Mizutani, M. Kato, J. Am. Ceram. Soc. 62 (1979) 219–224.
[25] Z.G. Liu, J.H. Ouyang, K.N. Sun, X.L. Xia, J. Power, Sources 195 (2010) 7225–7229.
[26] V.P. Kumar, Y.S. Reddy, P. Kistaiah, G. Prasad, C.V. Reddy, Mater. Chem. Phys. 112 (2008) 711–718.
[27] Y.P. Fu, Cer. Internat. 34 (2008) 2051–2057.
[28] J. Plocharski, W. Wieczorek, Solid State Ion. 28–30 (1988) 979–982.
[29] K.S. Sibi, A.N. Radhakrishnan, M. Deepa, P.P. Rao, P. Koshy, Solid State Ion. 180 (2009) 1164–1172.
[30] A.R. West, Basic Solid State Chemistry, second ed., Wiley, New York USA, 1999, pp. 351–352.
[31] A.R. West, Basic Solid State Chemistry, second ed., Wiley, New York USA, 1999, pp. 357–361.
[32] K. Kobayashi, M. Mukaida, T. Tsunoda, Y. Imai, Solid State Ion. 154–155 (2002) 101–107.